Scientific Research Publishing

Materials Sciences and Applications, 2026, 17(8), 231-240
https://www.scirp.org/journal/msa
ISSN Online: 2153-1188
ISSN Print: 2153-117X

The Effect of La Doping on the CO_2 Adsorption Properties of Silica: A Study of Adsorption Mechanisms Based on Crystal and Microporous Structures

Masanori Kobayashi

Department of Physical Therapy, College of Life and Health Sciences, Chubu University, Kasugai, Japan
Email: chubukoba@fsc.chubu.ac.jp

How to cite this paper: Kobayashi, M. (2026) The Effect of La Doping on the CO_2 Adsorption Properties of Silica: A Study of Adsorption Mechanisms Based on Crystal and Microporous Structures. *Materials Sciences and Applications*, **17**, 231-240.
https://doi.org/10.4236/msa.2026.178015

Received: July 1, 2026
Accepted: August 18, 2026
Published: August 21, 2026

Copyright © 2026 by author(s) and Scientific Research Publishing Inc.
This work is licensed under the Creative Commons Attribution International License (CC BY 4.0).
http://creativecommons.org/licenses/by/4.0/

Open Access

Abstract

This study investigates the influence of lanthanum (La) doping on the CO_2 adsorption behavior of silica-based porous composites synthesized via a chemical solution method. Structural analyses using X-ray diffraction (XRD) and transmission electron microscopy (TEM) confirmed that crystallization of lanthanum oxide within the amorphous silica matrix progresses with increasing La content. CO_2 adsorption measurements revealed that samples with lower La concentrations exhibited higher reversible adsorption capacities at low temperatures, indicating that physical adsorption within microporous structures plays a more dominant role than chemical interactions. Enhancing CO_2 adsorption performance requires maximizing the effective active surface area through uniform dispersion of fine lanthanum oxide particles. However, the complex involvement of fluid behavior and thermal expansion at elevated temperatures suggests that temperature-dependent structural design is essential for practical applications.

Keywords

Silica, Lanthanum (La) Doping, CO_2 Adsorption, Physical Adsorption, Chemical Adsorption, Crystal Structure

1. Introduction

The efficient capture of carbon dioxide (CO_2), a major contributor to global warming, has become an urgent global challenge. Amorphous silica has attracted attention as a gas separation material because its Si-O-Si network structure can be tailored to achieve selective adsorption depending on the target gas species [1]. Pre-

vious studies have reported that doping silica with transition metals introduces functional adsorption sites, such as hydrogen adsorption-desorption sites [2]-[4]. Our earlier work also demonstrated that La-doped silica exhibits higher CO_2 adsorption capacity than silica doped with other metals [5].

Adsorption mechanisms are generally classified into physical adsorption and chemical adsorption. Physical adsorption is governed primarily by van der Waals forces and is reversible upon evacuation. The adsorption amount is strongly influenced by the surface area and microporous structure of the material. In contrast, chemical adsorption involves stronger interactions—such as hydrogen bonding or acid-base interactions—comparable to those responsible for compound formation, and is therefore typically irreversible. Chemical adsorption depends on the type and chemical state of the doped elements and their reaction products [6].

The overall CO_2 adsorption capacity of a material is determined by the combined contributions of these two mechanisms. However, the manner in which doped elements influence the balance between physical and chemical adsorption remains insufficiently understood. Therefore, this study aims to clarify how varying the amount of La doping affects both physical adsorption (related to porous structure) and chemical adsorption (related to CO_2 affinity) by analyzing the resulting crystal states and microstructures of La-doped silica composites.

2. Experimental Methods

2.1. Sample Preparation

La-doped silica porous composites were synthesized following the procedure described in our previous report [7]. Anhydrous ethanol and tetraethoxysilane (TEOS) were mixed under stirring while maintaining the mixture at 0˚C to prevent ethanol evaporation. $La(NO_3)_3{\cdot}6H_2O$ was added to achieve Si:La molar ratios of 2:1, 4:1, and 8:1. After complete dissolution, hydrogen peroxide was added, and the mixture was stirred for 2 h. The resulting gel was dried at 60˚C for one week, ground into powder, and stored in a desiccator.

Thermal analysis (TG-DTA) was conducted to determine the calcination temperature, which was set to 600˚C. Samples were heated at 2˚C/min to 600˚C, held for 3 h, and cooled at 5˚C/min. **Figure 1** shows the synthesis flow chart and sample appearance.

2.2. Characterization

2.2.1. Structural Analysis

XRD measurements were performed using a Rigaku RINT2500 diffractometer (Cu Kα radiation, 3 kW, 50 mA, $2\theta = 20–60°$). Microstructural observations were conducted using a JEOL JEM-4000FX TEM and a Hitachi S-4500 SEM.

2.2.2. CO_2 Adsorption Measurements

To measure CO_2 adsorption capacity, CO_2 adsorption experiments were con-

ducted on samples of pure silica and La-doped silica with different compositions using a fully automated gas adsorption analyzer (specific surface area and pore size distribution analyzer; AUTOSORB), based on the volumetric method.

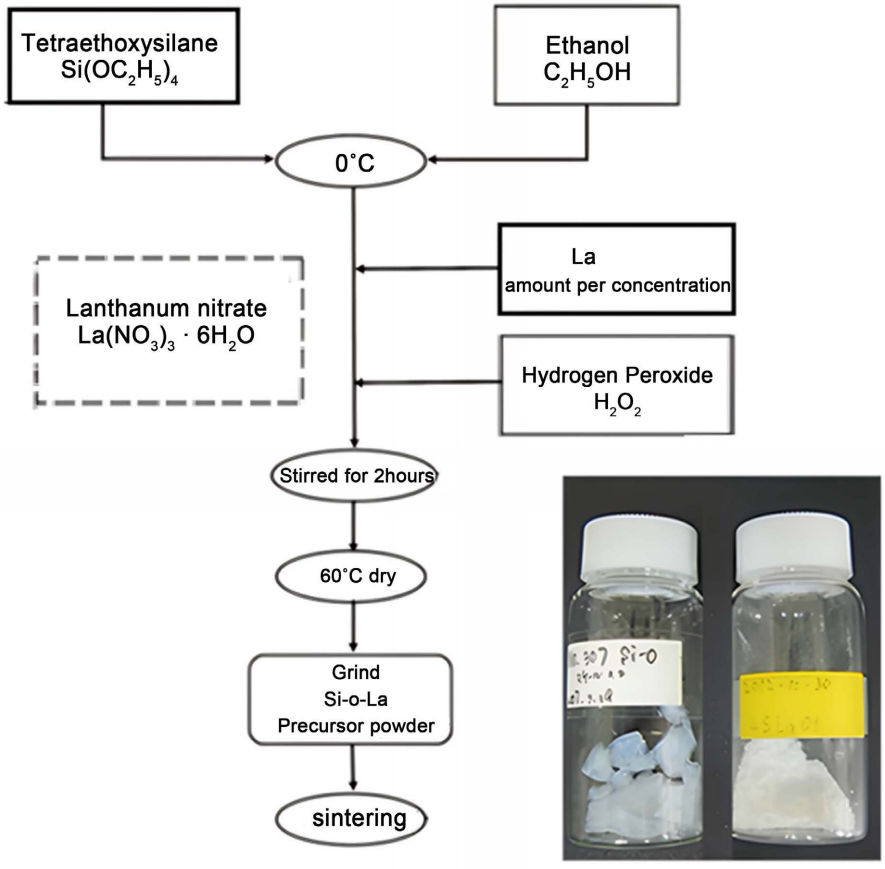

Figure 1. Flow chart of the production process of La-doped Silica specimen by a precursor solution method and sample views.

First, CO_2 was adsorbed onto the SiO_2-La composite sample by passing it through the sample under pressure. After holding the sample at this pressure for a set period, the CO_2 was desorbed by reducing the pressure, and the process was then repeated by reapplying pressure. For a sample under a single set of experimental conditions, this cycle was repeated several times; the amounts of gas adsorbed and desorbed during this process were measured, and the amount of gas adsorbed on the sample surface was determined based on these changes. The adsorption measurement is performed by opening a solenoid valve to introduce carbon dioxide from a manifold containing carbon dioxide at a specified pressure into the cell containing the sample. The amount of adsorption can be calculated from the difference between the amount of carbon dioxide introduced into the system and the amount of gas remaining in the system after adsorption.

Figure 2 shows a flowchart of the volumetric adsorption measurement apparatus.

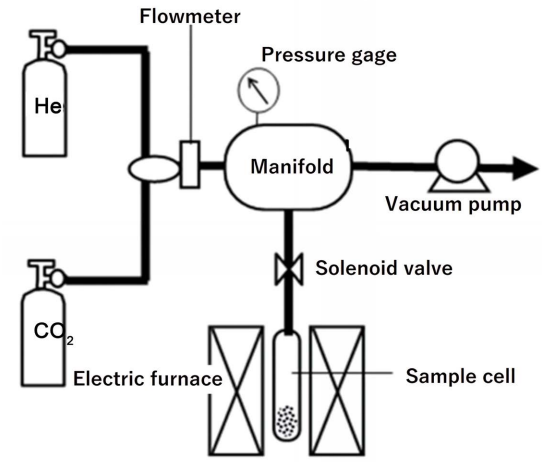

Figure 2. Flowchart for measuring carbon dioxide (CO_2) adsorption capacity using a AUTOSORB.

For two experimental temperatures—100˚C and 400˚C—we performed the same procedure on 20 to 25 samples at each temperature, varying the experimental pressure from 0 kPa to 110 kPa to obtain data on the pressure dependence of the CO_2 gas volume.

In AUTOSORB volumetric measurements, the amount of gas removed (*i.e.*, the amount adsorbed) can be calculated using the equation of state based on the "pressure change" before and after adsorption and the "known instrument volume" when gas is introduced from the manifold into the sample cell. In this way, the amount of CO_2 that can be measured by repeatedly performing desorption and adsorption under adsorption equilibrium pressure can be plotted at each pressure value at a constant temperature based on the actual material's adsorption system, generally yielding the adsorption isotherm shown in Figure 3.

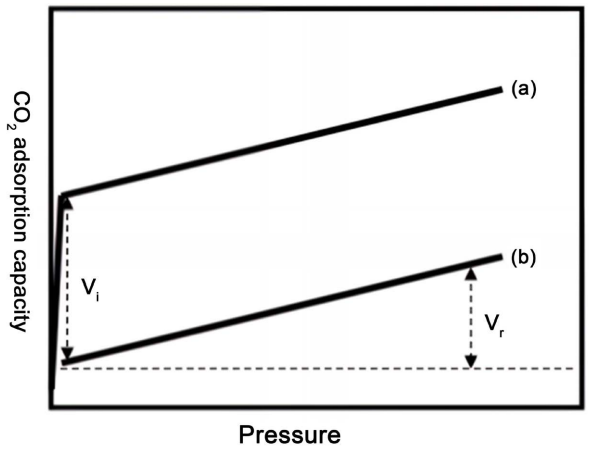

Figure 3. Carbon dioxide adsorption isotherms.

Line (a) shows the initial adsorption isotherm, while Line (b) shows the adsorption isotherm obtained after performing an adsorption measurement, followed by

a vacuum evacuation, and then conducting another adsorption measurement. The difference between these two adsorption isotherms (Vi) corresponds to the amount of carbon dioxide that is irreversibly adsorbed—that is, the amount of chemically adsorbed carbon dioxide—which cannot be desorbed at the measurement temperature due to strong adsorption forces.

On the other hand, the Vr shown in (b) corresponds to physical adsorption of carbon dioxide that can be reversibly adsorbed and desorbed in response to changes in carbon dioxide pressure. This analytical method has also been used in previous studies on CO_2 adsorption [8]. Possible sites for this adsorption include extremely small pores that can only be reached by gas diffusion, the interface between the support and the metal, or surface lattice defects.

3. Results

3.1. XRD Patterns of La-Doped Silica

Figure 4 shows the XRD patterns of samples with different La contents. The Si:La = 2:1 sample exhibited eight diffraction peaks corresponding to La_2O_3, indicating significant crystallization. The Si:La = 4:1 sample showed two La_2O_3 peaks ((002) and (011)), while the Si:La = 8:1 sample exhibited no distinct peaks, suggesting that La_2O_3 crystallization was suppressed and the amorphous silica structure was largely retained.

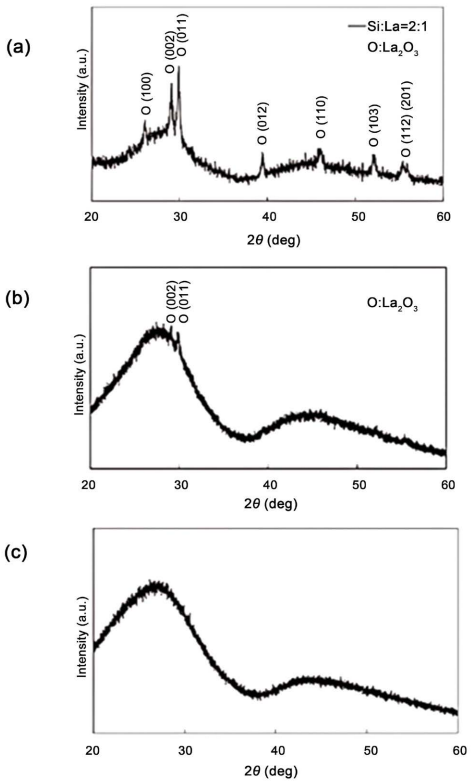

Figure 4. XRD pattern for the La-dope Silica specimens. (a) Si:La = 2:1; (b) Si:La = 4:1; (c) Si:La = 8:1.

3.2. Microstructural Observations

Although we did not perform SEM or TEM observations on all of the obtained samples, we did conduct microscopic observations on multiple specimens of each type. As a representative example, Figure 5 shows SEM and TEM images of a sample with a Si:La composition ratio of 4:1.

SEM (Figure 5(a)) revealed no obvious porous structure, although bright contrast regions were attributed to dispersed La_2O_3 particles. TEM analysis (Figure 5(b)) confirmed lattice fringes corresponding to La_2O_3 (100) and (012) planes.

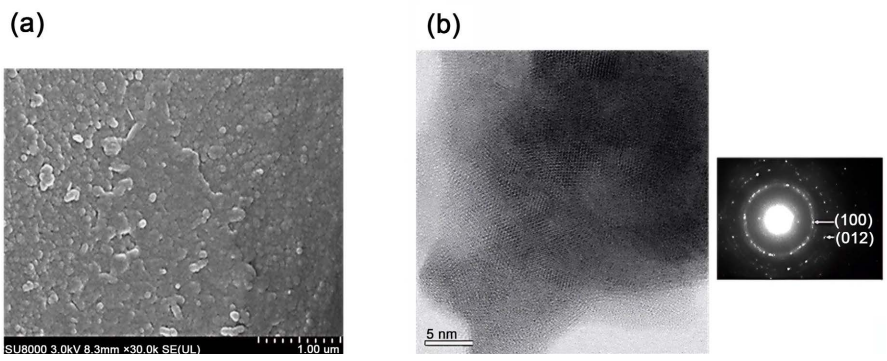

Figure 5. (a) SEM image and the electron diffraction pattern of La-dope Silica specimen; (b) TEM image and the electron diffraction pattern of La-dope Silica specimen (Si:La = 4:1).

3.3. CO_2 Adsorption Behavior

Figure 6 summarizes the CO_2 adsorption capacities. Pure silica exhibited negligible chemical adsorption, whereas La-doped samples showed measurable irreversible adsorption. However, in all samples, the proportion of chemical adsorption remained small, in dicating that physical adsorption dominated the overall CO_2 uptake.

Reversible adsorption showed strong temperature dependence. At 100˚C, lower La concentrations (Si:La = 8:1 and 4:1) yielded higher adsorption capacities. At elevated temperatures, adsorption decreased, except for the Si:La = 2:1 sample, which showed an anomalous increase at 400˚C.

The adsorption capacity varied significantly with temperature, and a temperature de pendence was confirmed. At the low temperature of 100°C, the higher the La doping level, the greater the reversible adsorption capacity; however, as the temperature increased, the CO_2 adsorption capacity tended to decrease.

The above results are summarized in Table 1.

4. Discussion

Except for the Si:La = 2:1 sample, La-doped silica exhibited higher CO_2 adsorption than pure silica, confirming that La contributes to enhanced adsorption performance. Previous studies have shown that La^{3+} increases surface basicity, strengthening CO_2-surface interactions and promoting chemical adsorption [9]-[11]. In

our samples, dispersed La_2O_3 particles likely served as chemical adsorption sites.

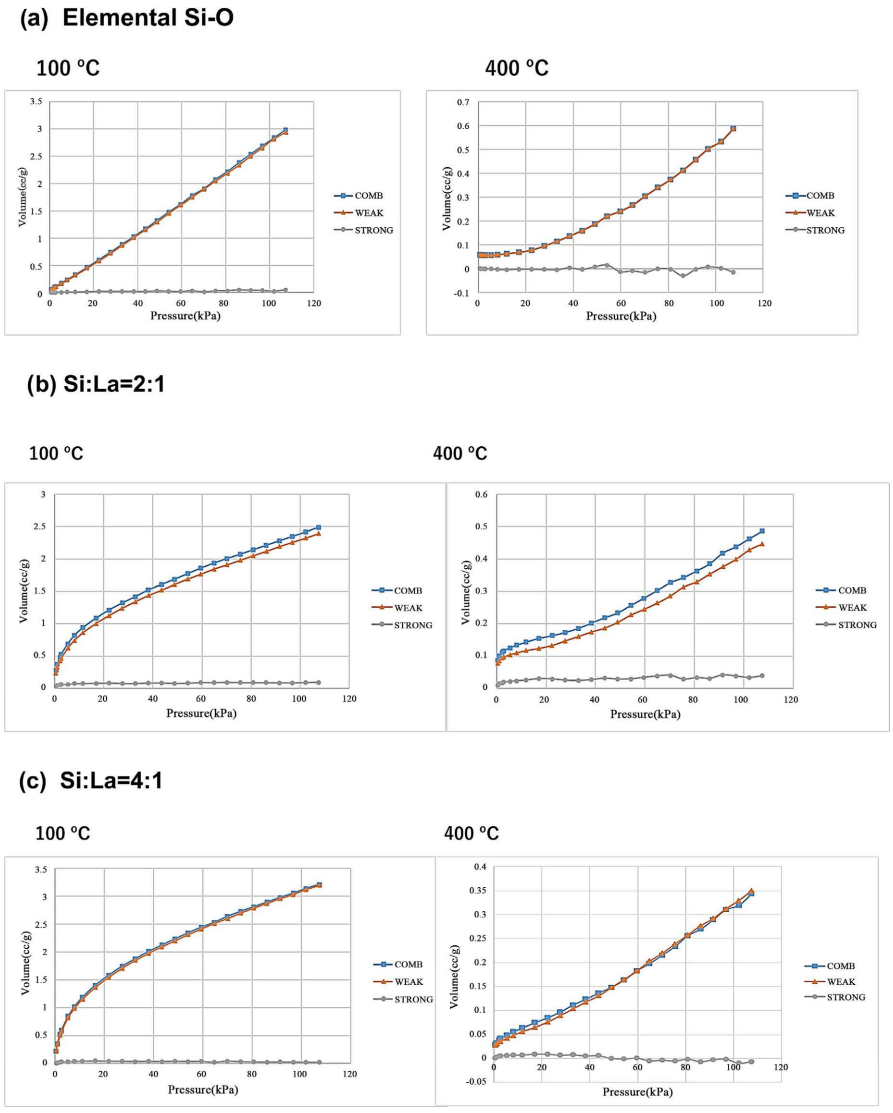

Figure 6. CO_2 adsorption capacities of various silica-lanthanum samples. (Weak: Reversible adsorption capacity, Strong: Irreversible adsorption capacity).

Table 1. Table summarizes the Average reversible CO_2 adsorption capacity (cc/g).

La-Concentration		Adsorption Temperature (˚C)	
n = 20 - 25	100˚C	200˚C	400˚C
SiO_2	2.7767	0.7098	0.7098
Si:La = 2:1	1.9587	0.71086	2.094
Si:La = 4:1	3.9206	1.81485	1.6764
Si:La = 8:1	5.14851	1.70202	1.03101

However, AUTOSORB measurements revealed that chemical adsorption con-

tributed only minimally to total CO_2 uptake. Instead, physical adsorption dominated, suggesting that La doping primarily influences the microstructural features that govern surface area and pore accessibility. SEM observations did not reveal macroscopic porosity, implying that structural changes occur at the nanoscale.

At high La concentrations (Si:La = 2:1), La_2O_3 crystallites grew larger, reducing effective surface area. In contrast, lower La concentrations (Si:La = 4:1 and 8:1) maintained smaller particle sizes, preserving microporous characteristics and enhancing physical adsorption.

Figure 7 illustrates the correlation between La content and the number of detectable La_2O_3 crystal planes. A greater variety of crystal planes during synthesis may promote the formation of diverse microstructural motifs within the amorphous silica matrix [12], facilitating the development of fine porous structures that enhance gas diffusion and trapping. This interpretation is consistent with insights from defect engineering [13].

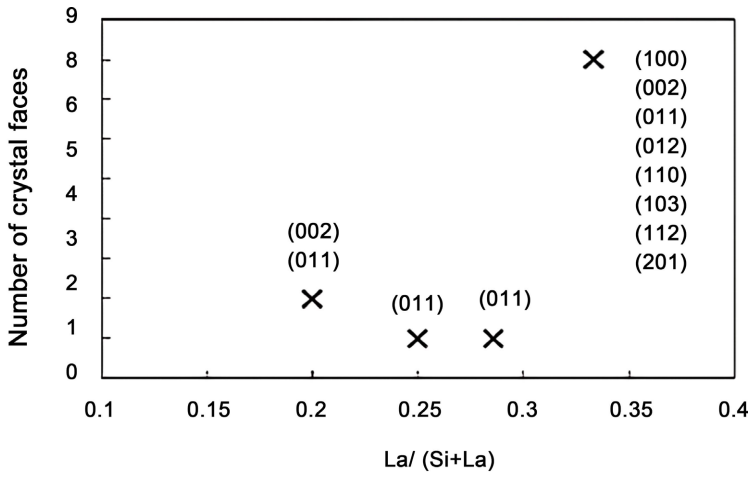

Figure 7. The correlation of the number of crystal faces and the amount of La in La-dope Silica specimen.

A limitation of this study is that we were unable to obtain direct evidence regarding the pore structure, such as the BET specific surface area or pore size distribution. In this regard, the author anticipates that much of what is discussed in this analysis will be subject to criticism, as it relies heavily on speculation and may appear somewhat illogical. However, the reality is that most CO_2 adsorption material development to date has not focused on crystal structure in this way; in that sense, I hope this work will lead to research and development from a new perspective such as effective active surface area and pore structure stability.

5. Conclusions

La-doped silica porous composites were synthesized via a chemical solution method, and the effects of La content on CO_2 adsorption behavior were evaluated. Increasing La content promoted La_2O_3 crystallization within the amorphous silica

matrix. CO_2 adsorption tests revealed that low La concentrations yielded higher reversible adsorption at low temperatures, indicating that physical adsorption within fine porous structures is the dominant mechanism.

Enhancement of CO_2 adsorption requires maximizing the effective active surface area through uniform dispersion of fine La_2O_3 particles. However, temperature-dependent structural changes and fluid behavior must be considered for practical applications. Future work should focus on detailed analysis of nanoscale structural features and fluid dynamics to guide the design of high-performance CO_2 adsorbents.

Acknowledgements

This study was conducted in collaboration with the Japan Fine Ceramics Center (JFCC). The author expresses sincere gratitude to Dr. Hiromi Ikuhara and the supporting staff for their valuable contributions.

Author Contributions

M.K. conceived and designed the study, performed the experiments, analyzed the data, and wrote the manuscript.

Conflicts of Interest

The author declares no conflicts of interest regarding the publication of this paper.

References

[1] Morimoto, N. (1989) Silica Minerals. In: *Igneous Mineralogy*, University of Tokyo Press. (In Japanese)

[2] Blanco, G., Calvino, J.J., Cauqui, M.A., Cifredo, G.A., Pérez Omil, J.A., Rodriguez-Izquierdo, J.M., *et al.* (1994) Characterization of Silica Dispersed Lanthana by CO_2 Adsorption. *Journal of Alloys and Compounds*, **207**, 201-205. https://doi.org/10.1016/0925-8388(94)90206-2

[3] Yoshioka, T., Maki, T., Asaeda, M. and Tsuru, T. (2007) Gas Permeation Properties of Metal-Doped Porous Silica Membranes Prepared by Sol-Gel Method for CO_2 Separation. *Membrane*, **32**, 45-53. (In Japanese)

[4] Ikuhara, Y.H., Saito, T., Sasaki, Y., Takahashi, S. and Hirayama, T. (2010) Determination of Reversible Hydrogen Adsorption Site in Ni-Nanoparticle-Dispersed Amorphous Silica for Hydrogenseparation at High Temperature. *Journal of Materials Research*, **25**, 2008-2014. https://doi.org/10.1557/jmr.2010.0254

[5] Kobayashi, M. and Koide, T. (2014) Synthetic Study and Structural Analysis of La-Doped Mi Croporous Silica Composites. *Bulletin of Daido University*, **50**, 73-77. (in Japanese) https://daido.repo.nii.ac.jp/record/30/files/08_kobayashi.pdf

[6] Society of Indoor Environment Science (2010) Introduction to Indoor Environmental Science; 2.4 Behavior of Indoor Chemical Substances; 3.4.3 Deposition on and Re-Release from Wall Surfaces. (in Japanese) https://www.tdupress.jp/book/b350293.html

[7] Iwamoto, Y., Sato, K., Kato, T., Inada, T. and Kubo, Y. (2005) A Hydrogen-Permselective Amorphous Silica Membrane Derived from Polysilazane. *Journal of the European Ceramic Society*, **25**, 257-264.

https://doi.org/10.1016/j.jeurceramsoc.2004.08.007

[8] Siriwardane, R.V., Shen, M., Fisher, E.P. and Losch, J. (2005) Adsorption of CO_2 on Zeolites at Moderate Temperatures. *Energy & Fuels*, **19**, 1153-1159. https://doi.org/10.1021/ef040059h

[9] Garbarino, G., Wang, C., Valsamakis, I., Chitsazan, S., Riani, P., Finocchio, E., *et al.* (2017) Acido-Basicity of Lanthana/Alumina Catalysts and Their Activity in Ethanol Conversion. *Applied Catalysis B*: *Environmental*, **200**, 458-468. https://doi.org/10.1016/j.apcatb.2016.07.010

[10] Hong, J., Kobayashi, S., Kuwabara, A., Ikuhara, Y.H., Fujiwara, Y. and Ikuhara, Y. (2021) Defect Engineering and Anisotropic Modulation of Ionic Transport in Perovskite Solid Electrolyte $LI_XLA_{(1-x)/3}NbO_3$. *Molecules*, **26**, Article 3559. https://doi.org/10.3390/molecules26123559

[11] Sardo, M., Morais, T., Soares, M., Vieira, R., Ilkaeva, M., Lourenço, M.A.O., *et al.* (2024) Unravelling the Structure of CO_2 in Silica Adsorbents: An NMR and Computational Perspective. *Chemical Communications*, **60**, 4015-4035. https://doi.org/10.1039/d3cc05942a

[12] Noda, Y. (2017) Crystallography and Structural Properties: From Fundamentals to Applications. Uchida Rokakuho Publishing. (In Japanese)

[13] Fang, Z., Bueken, B., De Vos, D.E. and Fischer, R.A. (2015) ChemInform Abstract: Defect-Engineered Metal—Organic Frameworks. *ChemInform*, **46**, 7234-7254. https://doi.org/10.1002/chin.201531257